

TRACE ELEMENT DISTRIBUTIONS IN COMPACT TYPE A Ca-Al-INCLUSIONS (CAI) IN ALLENDE AND LEOVILLE: EVIDENCE FOR DISSOLUTION OF RELICT PEROVSKITE
 A.K. Kennedy, I.D. Hutcheon and G.J. Wasserburg. Lunatic Asylum, Division of Geological and Planetary Sciences 170-25, California Institute of Technology, Pasadena, CA 91125

The presence of relict grains in a CAI constrains models of precursor formation and the thermal history of the inclusion. If a relict phase that contains a large fraction of the trace element budget of an inclusion is undergoing dissolution during the early stages of crystallization, its presence may be detected by comparison of trace element (TE) distributions in the crystallizing phases and the TE distributions predicted from experimental TE partitioning studies. Kennedy *et al.* [1] measured REE abundances in melilite (Mel) in Type B1 CAI and found low concentrations in early crystallizing, low akermanite (Ak), Mel and higher concentrations in later crystallized, higher Ak (up to Ak40) Mel. These results are inconsistent with the continuously decreasing concentrations predicted by the partitioning experiments of Beckett *et al.* [2] and Kennedy *et al.* [1] suggested dissolution of TE-rich relict perovskite (Pv) was responsible. Compact Type A (CTA) are ideal natural systems for testing the hypothesis that Pv dissolution controls the distribution of TE in Mel because, CTA are essentially two component systems of Mel (> 75%) and spinel (Sp) and Mel should display the same relationship between Ak and TE as the experiments, and, CTA often contain more Pv than Type B1 CAI. We have examined two Allende CTA, 818G and Linus Jr., and one Leoville CTA, L575, that are metamorphosed to different degrees and that have different populations and distributions of Pv. We measured major element compositions by SEM with EDS and Ba, Hf, REE, Sr and Ti, using the PANURGE ion microprobe, with techniques and standards of [1]. Our data show dissolution of relict Pv controls the distribution of TE in Mel in CTA and that metamorphism affected TE partitioning in some CTA.

818G is the least metamorphosed CTA with large elongate Mel surrounding a core containing euhedral Sp, and Fassaite (Fass) and Pv (up to 100 μ m). Small (< 10 μ m) Pv are present in the Wark-Lovering rim. Mel in Linus Jr. occurs in two texturally distinct forms, elongate (50 x 100 μ m) crystals with undulose extinction, occasionally with cores which are optically discontinuous in polarized light and densely packed polygonal crystals with 120° intersections. Rare Ti-rich Fass fills interstices in the core of the inclusion. Pv occurs as (60 μ m) euhedral crystals and numerous small (< 10 μ m) rounded grains. Hibonite (Hib) occurs as small (< 15 μ m) laths. L575 shows the greatest evidence of metamorphism. Mel exhibits kink banding, sutured lobate grain boundaries, deformation twins, 120° crystal intersections and dense fracturing. Sp and Hib are intimately intergrown and Pv and Fass are rare in this inclusion. Mel analyzed in these CTA have small Ak ranges, in 818G Mel has Ak 22 - 30, in Linus Jr. Ak 11 - 19, and in L575 Ak 10 - 20. In Linus Jr. there is a general increase in Ak from the rim to the interior. This trend was not observed in L575.

Bulk REE concentrations for the three CTA, calculated from mineral modes and the REE concentrations of individual phases are ~10x chondritic (ch). 818G has a group I and Linus Jr. a group II REE pattern. L575 has a modified group III pattern, with a negative Yb anomaly, but a positive Eu anomaly. In 818G, Mel REE patterns vary between flat and LREE depleted and Pv and Fass are LREE depleted (fig 1). Fass in 818G has extreme LREE depletions, with La ~ 1 x ch and Lu ~ 80 x ch. Mel, Pv and Fass in Linus Jr. have similar REE abundances to the respective phases in 818G, but with higher LREE/HREE and positive Tm anomalies reflecting the group II REE pattern of this inclusion. Figure 2 shows REE patterns of Mel and Hib in Linus Jr. and L575. Mel from the optically discontinuous core of a large crystal in Linus Jr. has an unusually high chondrite normalized (c.n.) LREE/HREE ratio, La/Tm_{c.n.} > 2 compared with La/Tm_{c.n.} = 1 in most Mel. In L575 Mel has a positive Eu and negative Yb anomaly and is LREE depleted (fig. 2). Hib in Linus Jr. is LREE enriched, has a negative Eu anomaly and ~ 100 x ch LREE abundances (fig. 2). Hib in L575 is LREE enriched and has similar REE abundances to Mel (fig. 2) but not the negative Yb anomalies observed in Mel.

The abundances and partitioning of TE in the different phases in 818G and Linus Jr. is generally

consistent with crystal/melt equilibrium, however there is no relationship between Mel Ak and Ba, Hf, Ti, or REE (Fig. 3) in CTA. This behavior contrasts strongly with the data from Type B1 CAI and the experiments of Beckett *et al.* [1] which predict that with increasing Ak in Mel the trivalent REE concentrations decrease rapidly and the concentrations of Eu, a divalent REE, Ba and Ti, highly incompatible elements in Mel, should increase. Ba concentrations (10-100ppm) in Mel are much higher than expected from equilibrium partitioning [1] in a bulk inclusion with 20-30xch Ba. The REE are positively correlated with Ti in Mel (Fig. 4), the opposite of the relationship expected. Cores of large Mel in the less metamorphosed region of Linus Jr. with high LREE/HREE may reflect the presence of relict unmetamorphosed Mel. These observations clearly demonstrate that TE were not homogeneously distributed in the melt during crystallization of Mel. The enrichment of Ti and REE in Mel reflects enrichment in the parent melt.

Dissolution of heterogeneously distributed relict Pv during Mel crystallization can explain both the localized melt enrichment of Ti and REE and the lack of a relationship between Ak and TE in Mel. Mel crystallized from a melt enriched by dissolution of relict Pv with similar REE concentrations to the Pv in the CTA should plot along the mixing line shown in fig 4. The Mel from the CTA do not plot along this line. This could result from higher REE abundances in relict Pv than the CTA Pv. Our data show that TE distributions in Mel in both Type B1 and CTA CAI often reflect dissolution of relict Pv during crystallization of Mel.

References: [1] Kennedy *et al.* (1990) LPS XXI, 621. [2] Beckett *et al.* (1990) GCA 54, 1755.

Figure 1: REE patterns of Pv, Mel and Fass in 818G.
Figure 2: REE patterns of Mel and Hib from Linus Jr. and L575.

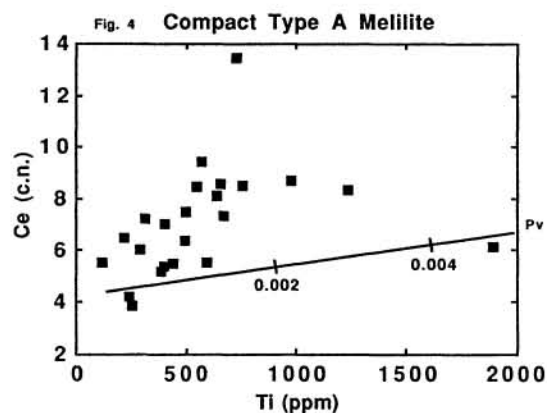
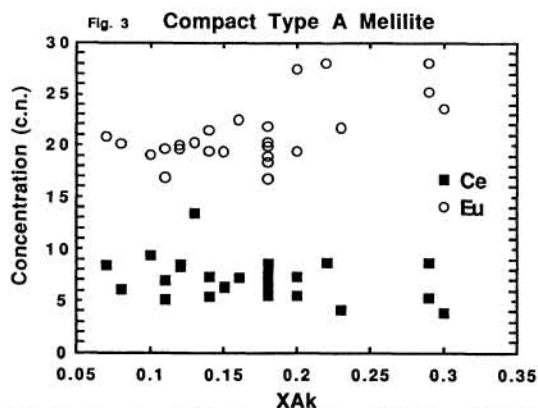
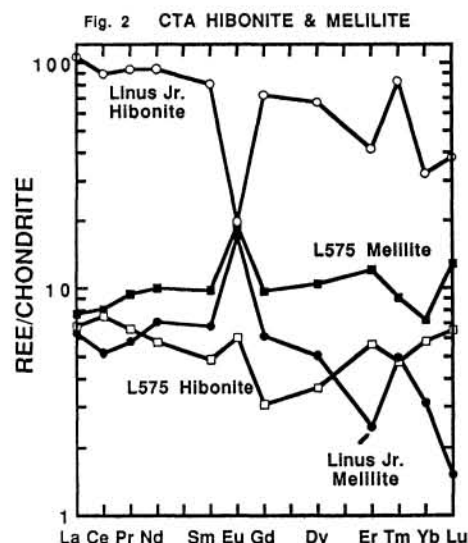
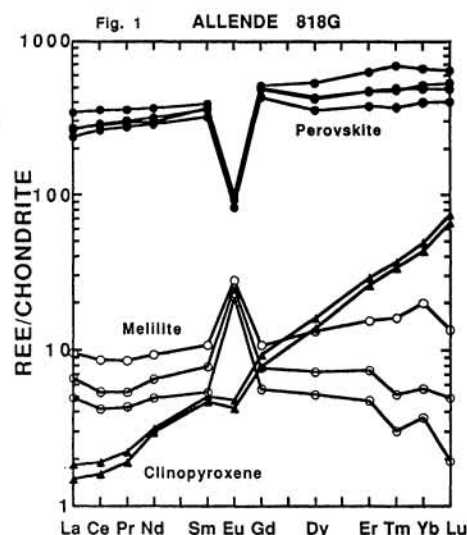


Figure 3: Ce (c.n.) and Eu (c.n.) vs. the XAK in CTA Mel. Figure 4: Ce (c.n.) vs. Ti (ppm) in CTA Mel. A mixing line between Mel, with 4.2xch Ce, and Pv, with 350xch Ce, labelled tick marks give the proportion of Pv in the mixture.